

Numerical modeling of the thermal conduction process in water-air convector's fins

Zhivko Kolev^{1,*}, and Seher Kadirova²

¹University of Ruse, Department of Heat, Hydraulics and Environmental Engineering, 7017 Ruse, Bulgaria

²University of Ruse, Department of Electronics, 7017 Ruse, Bulgaria

Abstract. The paper presents results from numerical modelling of thermal conduction process in ABAQUS. The computing mesh of the model has been verified. Based on the simulation results, the average temperature of the heat exchanger's external surface and the external heat convection coefficient have been determined. The process of thermal conduction in the fins is modelled on the basis of boundary conditions, which values are obtained by simulation of the heat convection process in the convector's pipes. The average heat parameters have been determined relative to the first, middle and last fins, by developing a geometric model in ABAQUS. The computing mesh has been verified by increasing the number of cells and nodes. The external heat convection coefficient is calculated by Newton's law.

1 Introduction

The processes of thermal conduction and the determination of their parameters have been studied in various fields. In [1] the thermal conductivity of building composite materials has been investigated. The thermal conductivity coefficient of the materials has been determined by TCi Mathis Thermal Conductivity Analyzer for non-destructive measurements. The mass specific heat capacity of the materials has been also determined. The paper presents investigation of thermal-physical characteristics of environmentally friendly building materials made by clay, sand and straw. Paper [2] presents determination of the heat capacity, thermal conductivity and thermal diffusivity of linalool - ethanol - water solutions. The purpose is determination of physicochemical and thermal properties of solutions with different ethanol concentrations, in order to describe the stability of the system. Heat transfer in thin plates with temperature dependent conductivity, has been considered in [3]. Due to the small thickness of the plates, two-dimensional modeling has been used. Graphical dependences of the thermal conductivity coefficient on the temperature of the plates are built. Investigation [4] presents numerical study of transient heat transfer process in longitudinal fins with different profiles. In the numerical models, linear or nonlinear functions of the temperature for the heat transfer coefficient and thermal conductivity coefficient have been used.

* Corresponding author: zkolev@uni-ruse.bg

Many papers present investigations of heat transfer processes in finned tube exchangers. In [5] heat transfer and flow characteristics of air over flat finned tubes, have been determined. Non-perforated fins and perforated with different shapes fins, have been investigated. The aim is determination of effective passive techniques for thermal performance enhancement of finned heat exchangers. Paper [6] presents experimental study of heat transfer in cross-flow heat exchanger with smooth tubes or integral finned tubes. The heat flow, heat transfer coefficient and overall heat transfer coefficient, have been determined at different velocities of the water flow in tubes, and different velocities of the air flow, which crosses the tubes. Experimental investigation of spiral finned tube heat exchanger has been considered in [7]. Different fin pitch, fin height, transverse tube pitch, and longitudinal tube pitch, have been investigated. The heat transfer Nusselt number and the flowing resistance Euler number, have been determined at different fluid flowing Reynolds number. Another research presents determination of the heat transfer coefficient of longitudinal finned tubes [8]. The local heat transfer coefficient and the temperature distribution have been determined for various Reynolds numbers of the fluid flow. In [9] a fin and tube heat exchanger has been studied by numerical modeling method. The gas flowing over the fin side is simulated at constant internal tube wall temperature, and the temperature distribution in the fins and the fluid velocity profile, have been determined. Paper [10] presents experimental study of the convective heat transfer process in finned tube counter flow heat exchanger. The convection heat transfer coefficient has been determined for plain tube, two finned tube and three finned tube. The investigation has been accomplished by different compositions of the liquid flowing in the pipes, at different Reynolds numbers. Numerical modeling of cross flow heat exchanger with louvered fins has been considered in [11]. A numerical model has been developed based on the thermal resistance concept and the finite difference method. Investigation [12] presents simulation study of a finned-tube latent heat thermal energy storage system. Numerical method based on heat capacity formulation, has been used for investigation of the influence of the convection heat transfer on the processes in the storage system. In [13] numerical simulation of the heat transfer in finned tube heat recovery unit, is considered. A method based on fluid-solid coupling is used for calculation of some parameters for the heat transfer process between the tube and the fluids. Paper [14] presents numerical study of circular tube bank fin heat exchanger with vortex generators. The fin's temperature distribution and the fluid's velocity distribution have been determined by simplified 3D model. CFD simulation investigation of the heat transfer in the pipes of water-air convector is considered in [15]. Pipe's sections with reduced heat transfer intensity, have been investigated.

The numerical modeling of heat transfer processes is related to determination of the temperature field [15-17]. ABAQUS is used in [15] and [16], while in [17] the used software product is ANSYS FLUENT.

The investigation of heat transfer processes in the heat consumers of heat pump installations is important, in terms of the wide-ranging use of the heat pumps for different needs [15, 18-21]. An experimental reversible water-to-water heat pump installation for air-conditioning is considered in [15] and [18]. The operation of air-to-water heat pump system for building's heating, has been investigated in [19]. In [20] and [21] mechanical vapor recompression heat pump for treatment of industrial wastewater, has been investigated.

For determination of certain parameters, in some cases it is necessary to study a sequence of heat transfer processes. The paper presents investigation of thermal conduction processes in the fins of water-air convector. The study has been accomplished in heating regime of the laboratory heat pump installation. The convector is used as a heat consumer. The temperature field in several fins of the convector's heat exchanger has been modelled, based on the results obtained from numerical modelling of heat transfer process in the

convector's pipes [15]. The temperature distribution results in the convector's fins have been used for determination of the heat convection coefficient ($h_{c-external}$, W/m².K) between the heat exchanger's external surface and the air flow. For this purpose, the average temperature of the surface (\bar{t}_w , °C) has been calculated. The calculations are on the base of two types of simulation results. One of them is the temperature field along the internal surface of the pipes. The other one is the temperature results for the heat exchange surface of three fins along the heat exchanger. The investigated fins are the first (№1), the middle (№79) and the last one (№157), respectively.

2 Methodology

2.1 Principal scheme of heat exchanger

Figure 1 presents a principal scheme of the convector's heat exchanger. It is two-pipe staggered finned pipe sheaf. When the heat pump installation operates in heating mode, the heat flow is transferred from the water flow in the pipes to the ambient air. The first row of finned pipes in the direction of air flow has been investigated.

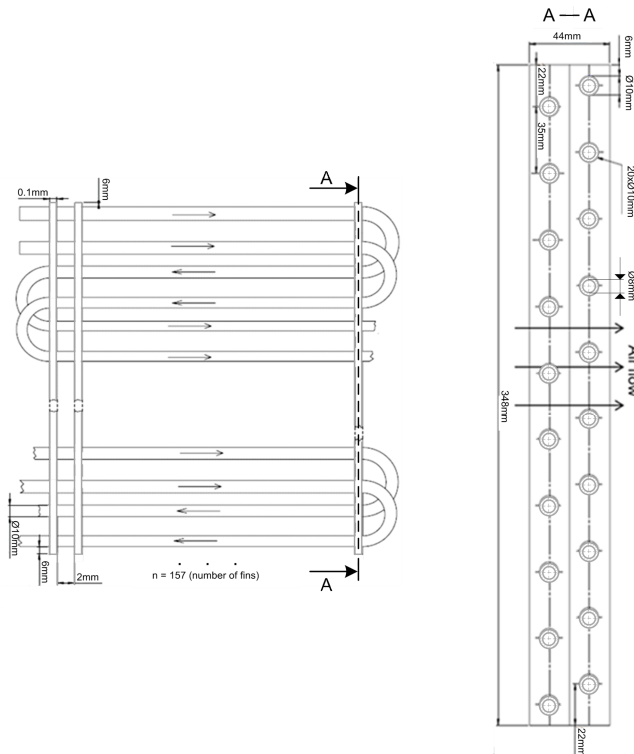


Fig. 1. Principal scheme of heat exchanger.

2.2 Schematic diagram of the simulation model

Figure 2 presents a schematic diagram of the numerical model for simulation of the temperature field in the convector's fins. For this purpose, the heat flux (q , W/m²) from the heat exchange surface to the environment, and the average temperatures of the fins' internal

cylindrical surfaces ($t_{w-1(I)} \div t_{w-4(X)}$, °C), have been set as boundary conditions. The temperature values have been determined from the simulation of the heat transfer process in the convector's pipes.

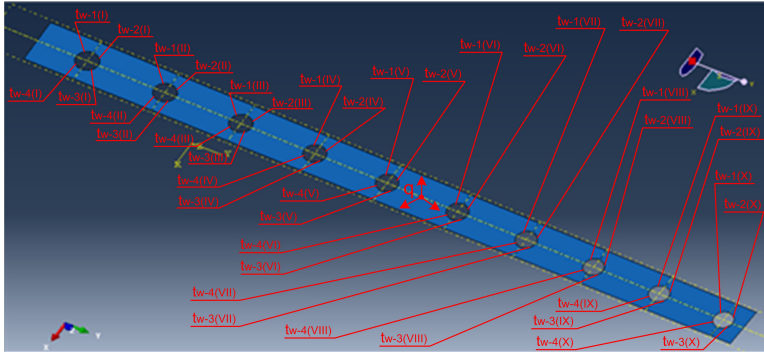


Fig. 2. Schematic diagram of the simulation model.

2.3 Verification of computing mesh

The verification of computing mesh has been performed using two temperatures (t_1 and t_2 , °C), defined for computing nodes. They are located on two of the edges of the middle fin (Fig. 3). Since the thermal resistance of the fin's wall is negligible, it is assumed that these are the values of the temperatures of the edges' nodes, located on the fin's opposite side.

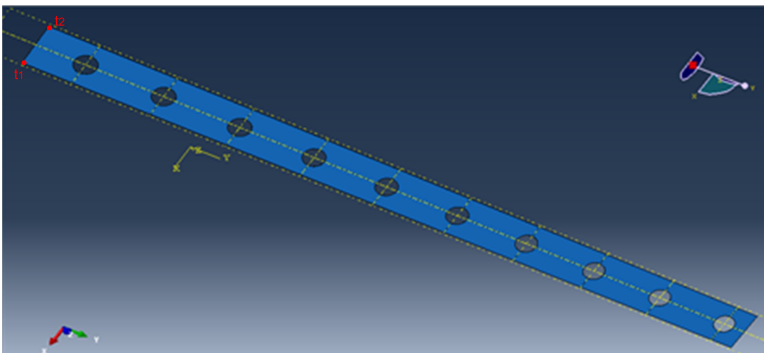


Fig. 3. Temperature points for verification of computing mesh.

2.4 Calculation of the heat convection coefficient

The heat convection coefficient between the heat exchanger's external surface and the air flow has been calculated by (1):

$$\overline{h_{c-extermal}} = \frac{q}{t_w - t_{heated\ air}} \tag{1}$$

where $\overline{t_{heated\ air}}$ is the average temperature of the air, heated by the exchanger's external surface, °C. This temperature has been calculated on the base of the basic heat equation, using experimentally determined parameters of the heat pump installation.

3 Results and discussion

3.1 Results from determination of the boundary conditions

Figures 4 - 6 present results obtained for the temperature field in the convector's pipes. They are base for calculation of the average temperature of the external cylindrical surfaces of the pipes between the fins, and the temperatures $t_{w-1(l)} \div t_{w-4(x)}$. The temperatures $t_{w-1(l)} \div t_{w-4(x)}$ are boundary conditions for simulation the thermal conduction process in the three investigated fins.

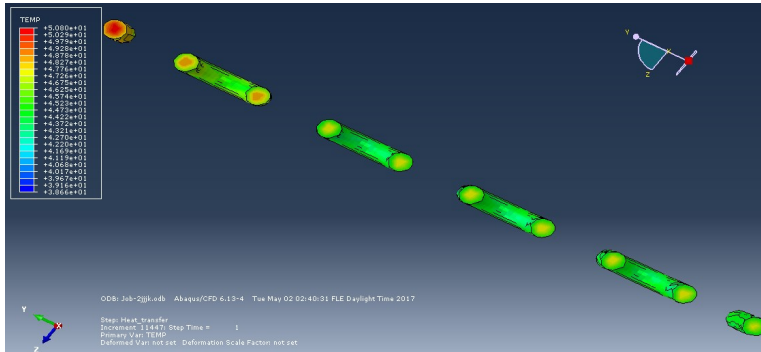


Fig. 4. Temperature field of the fluid – cross-section in the middle of the first fin.

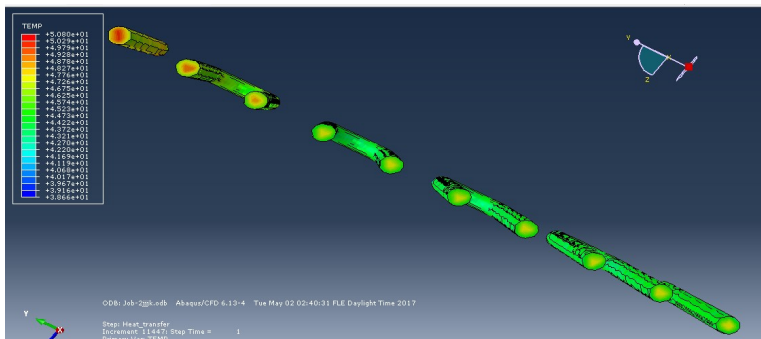


Fig. 5. Temperature field of the fluid – cross-section in the middle of the middle fin.

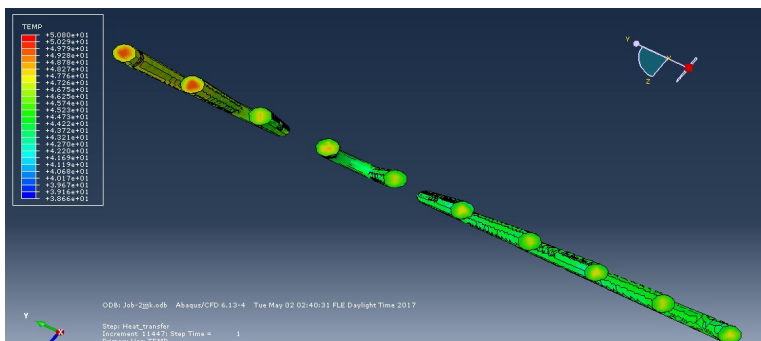


Fig. 6. Temperature field of the fluid – cross-section in the middle of the last fin.

In these simulations, „Tet” shape of the computing cells is set. The approximate size of the cells is 0.005 m. The number of computing cells is 69293, and the number of computing

nodes is 18384. The used turbulent model is „Spalart–Allmaras”. The obtained temperature field of the fluid presents the heat transfer intensity in different sections of the pipes.

Tables 1 – 3 present the values of the temperatures, used as boundary conditions for simulation the thermal conduction process in the three fins. The first row of the tables gives information about the number of the pipe’s cross-sections. The average heat flux q is 1108.79 W/m^2 , and is with constant value for all fins. The value of heat flux has been determined by calculations of the heat transfer process in the convector’s pipes.

Table 1. Temperature values for simulation of the first fin.

	I	II	III	IV	V	VI	VII	VIII	IX	X
$t_{w-1}, \text{ }^\circ\text{C}$	48.109	45.511	44.990	44.188	44.271	44.061	44.169	44.162	43.918	44.293
$t_{w-2}, \text{ }^\circ\text{C}$	47.912	46.242	46.005	44.500	44.723	44.641	45.009	44.533	44.929	44.237
$t_{w-3}, \text{ }^\circ\text{C}$	47.582	45.714	46.300	44.111	44.879	44.405	44.883	44.321	44.936	44.218
$t_{w-4}, \text{ }^\circ\text{C}$	47.862	45.392	45.578	44.183	44.275	44.042	44.188	44.123	44.166	44.079

Table 2. Temperature values for simulation of the middle fin.

	I	II	III	IV	V	VI	VII	VIII	IX	X
$t_{w-1}, \text{ }^\circ\text{C}$	47.559	46.387	45.444	44.411	44.317	44.479	44.685	44.425	44.220	44.207
$t_{w-2}, \text{ }^\circ\text{C}$	46.516	46.364	45.536	44.767	44.301	44.572	44.292	44.940	44.231	44.059
$t_{w-3}, \text{ }^\circ\text{C}$	46.943	45.807	45.240	44.514	44.239	44.098	44.169	44.167	44.057	44.099
$t_{w-4}, \text{ }^\circ\text{C}$	47.569	45.947	44.910	44.505	44.181	44.167	44.462	43.705	43.969	44.197

Table 3. Temperature values for simulation of the last fin.

	I	II	III	IV	V	VI	VII	VIII	IX	X
$t_{w-1}, \text{ }^\circ\text{C}$	46.879	46.150	44.999	44.139	44.279	43.848	44.111	43.744	44.557	43.883
$t_{w-2}, \text{ }^\circ\text{C}$	47.174	46.694	45.164	45.207	44.267	43.556	44.344	44.389	44.369	44.718
$t_{w-3}, \text{ }^\circ\text{C}$	46.859	47.222	45.056	45.338	44.193	44.618	44.392	44.614	44.592	44.908
$t_{w-4}, \text{ }^\circ\text{C}$	46.498	46.076	45.096	44.553	44.415	43.956	44.373	43.612	44.507	44.745

The presented temperatures are obtained from the average values in the respective computing nodes in the internal surface of the pipes. The temperatures are highest in the first cross-section, because there the temperature of the fluid flowing in the pipe is the highest.

3.2 Results from verification of computing mesh

Table 4 presents the results from verification of computing mesh. The differences in temperature values have been calculated by subtracting of the down row values from the up row values in each column of the table. The selected shape of computing cells is “Hex (sweep)”.

Table 4. Results from verification of computing mesh.

Mesh	Cell's size, m	Number of cells	t_1 , °C	Difference of t_1 , °C	t_2 , °C	Difference of t_2 , °C
I	0.01000	220	30.1896	-	30.1470	-
II	0.00800	238	30.1365	0.0531	29.9749	0.1721
III	0.00700	258	30.1168	0.0197	29.9467	0.0282
IV	0.00600	282	29.7362	0.3806	29.6725	0.2742
V	0.00500	320	29.7321	0.0041	29.6640	0.0085
VI	0.00450	356	29.5580	0.1741	29.4934	0.1706
VII	0.00400	463	29.3519	0.2061	29.2850	0.2084
VIII	0.00350	517	29.1894	0.1625	29.1871	0.0979
IX	0.00335	613	29.3248	-0.1354	29.2689	-0.0818

From the data presented in the table it can be seen that the tendency is to increase the values of temperatures t_1 and t_2 , until reaching of computing mesh IX. The change of temperatures with increasing mesh density is presented. On the base of the obtained results, computing mesh VIII has been selected. In Fig. 7 can be seen the number of cells and their specific shapes. The number of the nodes is 1312.

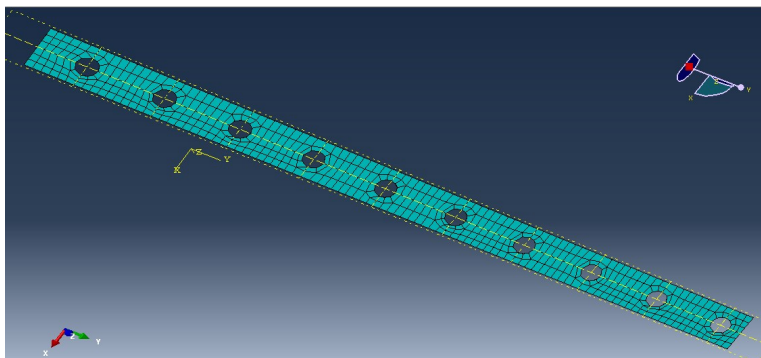


Fig. 7. View of selected computing mesh.

3.3 Simulation results for the temperature distribution in fins

Figures 8 - 10 present the simulation temperature fields obtained for the three fins. The presented temperature distribution expresses the heat transfer intensity between the respective zones of the fins and the air flow. It can be seen that the temperatures of the fins' areas, located at the greatest distance from the pipes, are the lowest.

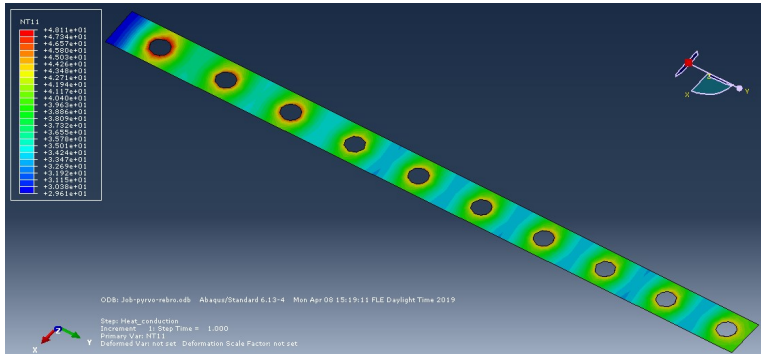


Fig. 8. Veiv of the temperature field in the first fin.

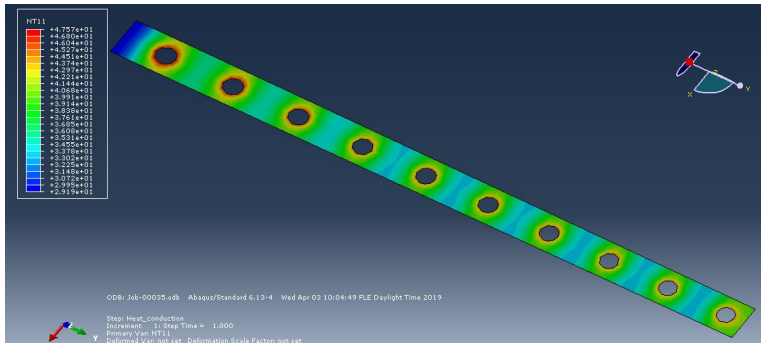


Fig. 9. Veiv of the temperature field in the middle fin.

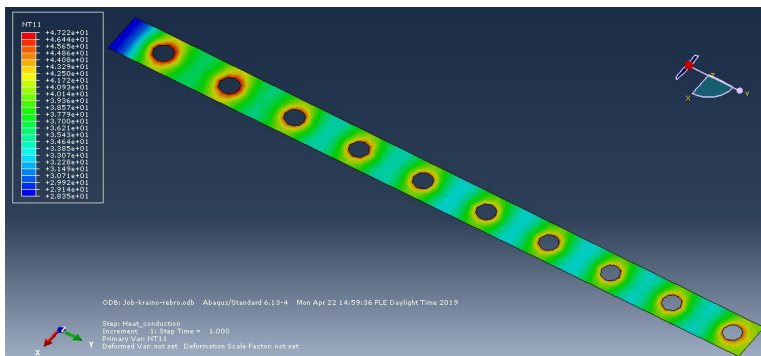


Fig. 10. Veiv of the temperature field in the last fin.

3.4 Results for the average temperatures and heat convection coefficient

Table 5 presents the calculated results for the following parameters: average temperatures of the heat exchange surfaces of the fins, average temperature of the heat exchanger's external surface, and external heat convection coefficient.

Table 5. Results for the calculated parameters.

$\bar{t}_{w-first_fin}$, °C	$\bar{t}_{w-middle_fin}$, °C	\bar{t}_{w-last_fin} , °C	\bar{t}_w , °C	$\bar{t}_{heated\ air}$, °C	$h_{c-external}$, W/(m ² .K)
38.492	38.319	38.387	39.386	19.662	56.215

The ambient temperature during the investigation has been 14.2 °C.

The relatively small difference in the average temperatures of the studied fins is an indicator of a relatively small difference in the amount of heat they exchange with the air flow crossing them.

For comparison of the results presented in Table 5 with results obtained by another method, the heat convection coefficient of the two-pipe sheaf is calculated, based on a criterion equation. The value obtained is 40.737 W/m².K. It should be noted that the data in Table 5 refer to the first row of the sheaf.

4 Conclusions

A methodology for determination of the external heat convection coefficients of finned water-air heat exchangers has been developed. The methodology is consist of numerical modeling of the heat convection processes in the ducts and subsequent numerical modeling of the thermal conduction processes in the fins.

Schematic diagram of the simulation model has been built in ABAQUS. The model has been developed, and the computing mesh has been verified.

The temperature field of the pipes' external heat exchange surface has been obtained by ignoring the thermal resistance of the pipes walls.

The average temperature of the convector's external heat exchange surface has been calculated based on the temperature field of the pipes' external surface in the zones between the fins, as well as based on the fins' temperature field.

The average external heat convection coefficient has been calculated on the base of the average temperature of the heat exchanger's external surface.

The big number of temperatures used as boundary conditions to simulate the process of thermal conductivity in the fins is a prerequisite for accurate determination of the simulation temperature field.

The developed methodology allows the results obtained in the first simulation to be used as boundary conditions for the implementation of the second simulation. Thus, the temperature field in the fins of the heat exchanger can be obtained, given the existing difficulties in measuring the maximum number of temperatures and its experimental building.

The precise determination of the external heat convection coefficient is very important, given the fact that it has a higher impact on the overall heat transfer coefficient of the investigated heat exchanger.

References

1. R. Petkova-Slipets, P. Zlateva, Thermal insulating properties of straw-filled environmentally friendly building materials, *De Gruyter*, 52 (2017)
2. S. Tasheva, V. Gandova, K. Dobreva, I. Dincheva, V. Prodanova-Stefanova, A. Stoyanova, Studies of physicochemical and thermal properties of linalool-ethanol-water system, *Research Journal of pharmaceutical, Biological and Chemical Science*, **10** (6), 220 (2019)
3. R. M. Saldanha da Gama, F. B. de Freitas Rachid, M. L. Martins-Costa, Mathematical modeling of heat transfer problems in thin plates with temperature dependent conductivity, *Heat Transfer Research*, (2017)
4. N. Namdari, M. Abdi, H. Chaghomi, F. Rahmani, Numerical solution for transient heat transfer in longitudinal fins, *International Research Journal of Advanced Engineering and Science*, 131 (2018)

5. M. Zaidan, A. Alkumait, T. Ibrahim, Assessment of heat transfer and fluid flow characteristics within finned flat tube, *Case Studies in Thermal Engineering* **12**, 557 (2018)
6. Z. Kadhim, M. Kassim, A. Hassan, Effect of integral finned tube on heat transfer characteristics for cross flow heat exchanger, *International Journal of Computer Applications* (**0975 – 8887**), 139 (2016)
7. He Fa Jiang, Cao Wei Wu, Yan Ping, Experimental investigation of heat transfer and flowing resistance for air flow cross over spiral finned tube heat exchanger, *Energy Procedia* **17**, 741 (2012)
8. A. Cebula, T. Sobota, Determination of the heat transfer coefficient distribution on the longitudinal finned tubes in staggered arrangement using inverse and CFD method, *European Conference on Computational Fluid Dynamics (ECCOMAS CFD)*, (2006)
9. S. Singh, K. Sørensen, T. Condra, Multiphysics numerical modeling of a fin and tube heat exchanger, *Proceedings of the 56th SIMS*, 383 (2015)
10. M. S. Baba, M. Bhagvanth Rao, A. V. Sita Rama Raju, Experimental study of convective heat transfer in a finned tube counter flow heat exchanger with Fe₃O₄ – water nanofluid, *International Journal of Mechanical Engineering and Technology (IJMET)*, 500 (2017)
11. D. Jung, D. N. Assanis, Numerical modeling of cross flow compact heat exchanger with louvered fins using thermal resistance concept, *SAE Technical Paper Series*, (2006)
12. S. Arena, E. Casti, J. Gasia, L. F. Cabeza, G. Cau, Numerical simulation of a finned-tube LHTES system: influence of the mushy zone constant on a phase change behavior, *Energy Procedia* **126 (201709)**, 517 (2017)
13. Lin Wei, Guorong Zhu, Zhijiang Jin, Numerical simulation of heat transfer in finned tube of heat recovery unit using fluid-solid coupled method, *Advances in Mechanical Engineering*, (2015)
14. Shubham Singh, Venkata Krishnan K., Spandana H., Mahesh Kumar N., P. S. Kulkarni, Numerical study of the heat transfer enhancement of circular tube bank fin heat exchanger with vortex generators, *20th Annual CFD Symposium – Bangalore*, (2018)
15. Zh. Kolev, S. Kadirova, Numerical modelling of heat transfer in convector's pipes by ABAQUS, *IOP Conf. Series: Materials Science and Engineering*, 595 (2019)
16. Z. Kolev, S. Kadirova, CFD simulation of forced heat transfer of gas in pipe, *E3S Web of Conferences* **112**, 01008, TE-RE-RD (2019)
17. E. Dimofte, F. Popescu, I. Ion, Numerical modelling of mixing fluids at different temperatures, *Proceedings of TE-RE-RD*, 35 (2016)
18. Z. Kolev, S. Kadirova, T. Nenov, Research of reversible heat pump installation for greenhouse heating, *INMATEH - Agricultural Engineering*, 77 (2017)
19. P. Zlateva, K. Yordanov, Experimental study of heat pump type air-water for heating system performance, *E3S Web of Conferences* **112**, 01007, TE-RE-RD, (2019).
20. S. Valchev, N. Nenov, Determination of specific energy consumption of mechanical vapor recompression heat pump, *Scientific Researches of the Union of Scientists in Bulgaria – Plovdiv*, 99 (2016).
21. S. Valchev, N. Nenov, Study of thermodynamic parameters of mechanical heat pump system, *Scientific Works of University of Food Technologies*, 247 (2016)